

1. Introduction and problem statement

The water temperature of freshwater lakes is mainly influenced by surface heat fluxes. Temperature changes in turn affect the physical, chemical and biological states of the water body. Here, we consider the dynamic behavior of surface heat fluxes in a large aquatic system. We investigate the spatio-temporal patterns of lake surface water temperature (LSWT) for Lake Geneva, Switzerland (the largest lake in Western Europe), making use of bulk formulas.

The total heat exchange at the air-water interface is:

$$Q_{tot} = Q_{sw} + Q_{atm} + Q_{br} + Q_{ev} + Q_{co} + Q_{pr} + Q_{lo}$$

The right side terms describe solar short-wave radiation, atmospheric long-wave radiation, surface reflection, evaporation/condensation, convection, precipitation onto the water surface, and the effect of water inflows/outflows, respectively. Neglecting the effect of precipitation and throughflow in the heat flux modeling of large lakes leaves five major heat flux terms to consider. We employed commonly used formulas for inland waters (see Table 1). The total possible combinations of these formulas gives a total of 324 different total heat flux models, and 6 calibration factors. These 324 models were investigated with the aim:

- Determine the best model for computing the Lake Geneva's surface heat fluxes.

To achieve this aim, it was necessary to:

- Find the corresponding calibration factors for the different models.
- Calculate the surface heat fluxes by comparing model output to field data.

Table 1 Formulas used to compute surface heat flux [1-4].

Solar Radiation	$Q_{sw} = Q_{F_{sw}}(1 - A_{sw}) + Q_{F_{ref}}(1 - A_{ref})$, $F_{sw} = (1 - C)[(1 - C) + 0.5C]$, $F_{ref} = (0.5C)[(1 - C) + 0.5C]$ $Q_{sw} = (1 - r_s)Q_{F_{sw}}(C)$, $f_{sw}(C) = 1 - 0.65C$, $r_s = 0.06$ $Q_{sw} = (1 - r_s)Q_{F_{sw}}(C)$, $f_{sw}(C) = 1 - 0.4C - 0.38C^2$
Atmospheric Radiation	$Q_{atm} = (1 - A_a)E_a\sigma T_a^4$, $E_a = a(1 + C_{cloud}C^2)1.24\left(\frac{e_a}{T_a}\right)^{0.789+0.03477T_a}$, $e_a = e_{sat}23.38\exp\left(18.1 - \frac{5303.3}{T_a}\right)$ $Q_{atm} = (1 - A_a)E_a\sigma T_a^4$, $e_a = e_{sat}10^{1.0+0.004127C}$, C_{cloud} and a : Calibration factors $Q_{atm} = (218 + 6.3T_a)(1 + C_{cloud}C^2)$
Back Radiation	$Q_{br} = -0.972\sigma T_w^4$ $Q_{br} = -(1 - A_w)\epsilon_w\sigma T_w^4$ $Q_{br} = -(303 + 5.2T_w)$
Evaporation	$Q_{ev} = -f_{ev}L_v(e_a - e_w)$, $f_{ev} = a(4.4 + 1.82U_w + 0.26(T_w - T_a))$, $e_w = 6.112\exp\left[\frac{17.62T_w}{243.12 + T_w}\right]$ $Q_{ev} = -f_{ev}L_v(e_a - e_w)$, $f_{ev} = (3.5 + 2U_w)\left(\frac{5 \times 10^4}{S_{sat}}\right)^{0.001}$, $L_v = 2.5 \times 10^6 - 2.3 \times 10^3 T_w$ $Q_{ev} = -f_{ev}L_v(e_a - e_w)$, $f_{ev} = C_{ev}U_w + C_{ev,cal}$, $C_{ev,cal}$: calibration factor $Q_{ev} = -(Q_{ev,forced} + Q_{ev,free})$ where: $Q_{ev,forced} = -L_v D_a f(U_w)(q_w - q_a)$ and $Q_{ev,free} = -k L_v \bar{P}_a (q_w - q_a)$ $f(U_w) = C U_w + C'$; Dalton Number, Calibration factor, $k = C_{p,conv} \left[\frac{g D_a^2}{U_w \bar{P}_a} (\rho_w - \rho_a) \right]^{1/2}$, $D_a = \frac{U_w}{Pr}$
Convection	$Q_{co} = -\gamma f_{co}(T_w - T_a)$, $\gamma = 0.62 hPaK^{-1}$ $Q_{co} = -\gamma_2 f_{co}(T_w - T_a)$, $\gamma_2 = \frac{C_p P}{0.622 L_v}$ $Q_{co} = -(Q_{co,forced} + Q_{co,free})$ where: $Q_{co,forced} = -\rho_a C_p g(U_w)(T_w - T_a)$ and $Q_{co,free} = -k \bar{P}_a C_p (T_w - T_a)$ $g(U_w) = C U_w + C'$; Stanton Number, Calibration factor

2. Materials and methods

- Meteorological data from 2010 were taken from an operational numerical weather prediction model, namely COSMO-2 (run by the Swiss meteorological service, 2.2 km resolution), while Advanced Very High Resolution Radiometer (AVHRR, 1 km resolution) satellite imagery was used for the LSWT.
- The temporal evolution of the heat content, G , was estimated using long-term time series of vertical temperature profiles at two points in the lake (SHL2 and GE3, Fig. 1). The total surface heat flux and temporal variation of heat content then is calculated at the same points.
- Monte Carlo method was used to find the optimal calibration factors (1.5×10^5 random values for each model, hence $324 \times 1.5 \times 10^5 = 4.86 \times 10^7$ simulations in total).
- The obtained root mean square errors (RMSE) are compared to find the best combination of heat flux terms, and consequently the best model.

$$G_{obs}^n = \int_z \rho_w C_p T dz$$

$$Q_{tot,ijkpq}^n = Q_{sw,i}^n + Q_{atm,j}^n + Q_{br,k}^n + Q_{ev,q}^n + Q_{co,p}^n, i, j, k, q = 1:3, p = 1:4 \rightarrow G_{model}^n - G_{obs}^n = \int_{t_0}^t Q_{tot,ijkpq} dt$$

$$RMSE_{ijkpq} = \sqrt{\frac{\sum_{n=1}^N [(G_{obs}^n - G_{model}^n) - (G_{model}^n - G_{model}^n)]^2}{N}}$$

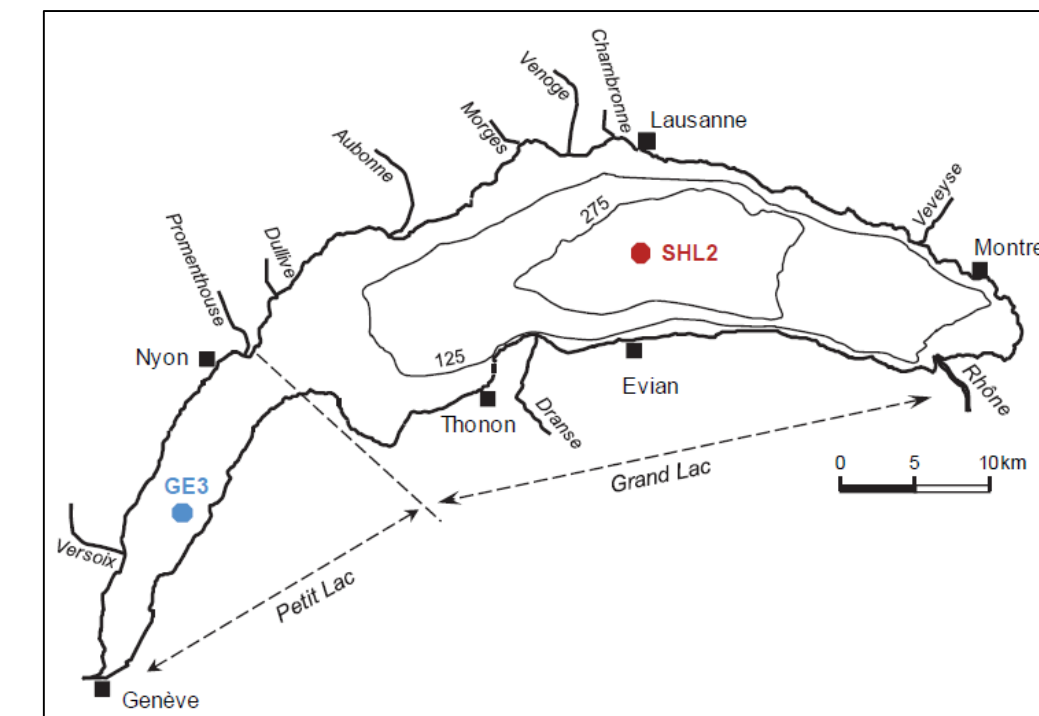


Figure 1. SHL2 and GE3 monitoring points (data from the *Commission Internationale de la Protection des Eaux du Léman*) located in Lake Geneva's large basin (*Grand Lac*) and small basin (*Petit Lac*), respectively.

3. Results: Model determination and temporal variation of total heat content

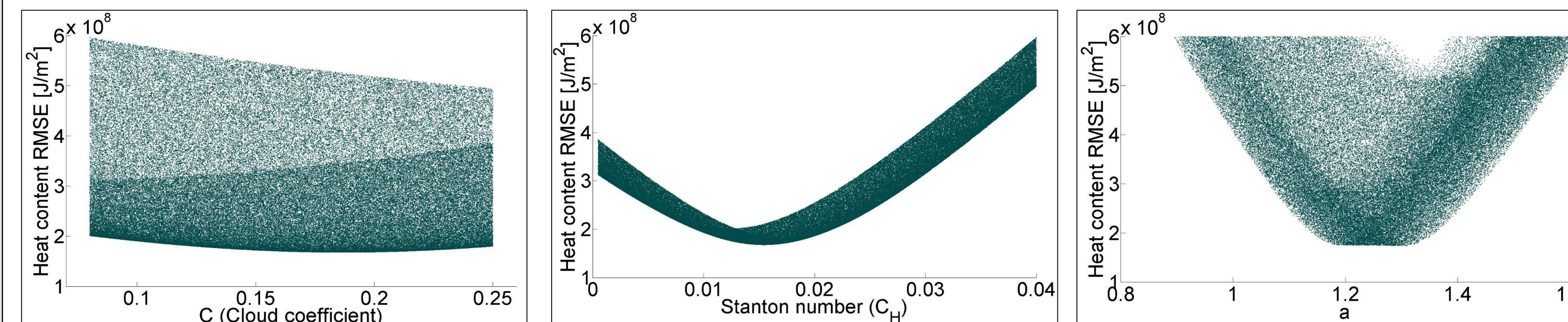


Figure 2 Example Monte Carlo simulation results used to tune the calibration factors for each heat flux model. For example, the optimum value of $C_{cloud} = 0.1869$ (left), the optimum value of $C_H = 0.0154$ (middle) for the best model, $Q_{tot,12313}$, and the optimal value of $a = 1.2977$ (right) for another good model, $Q_{tot,12313}$, are shown here.

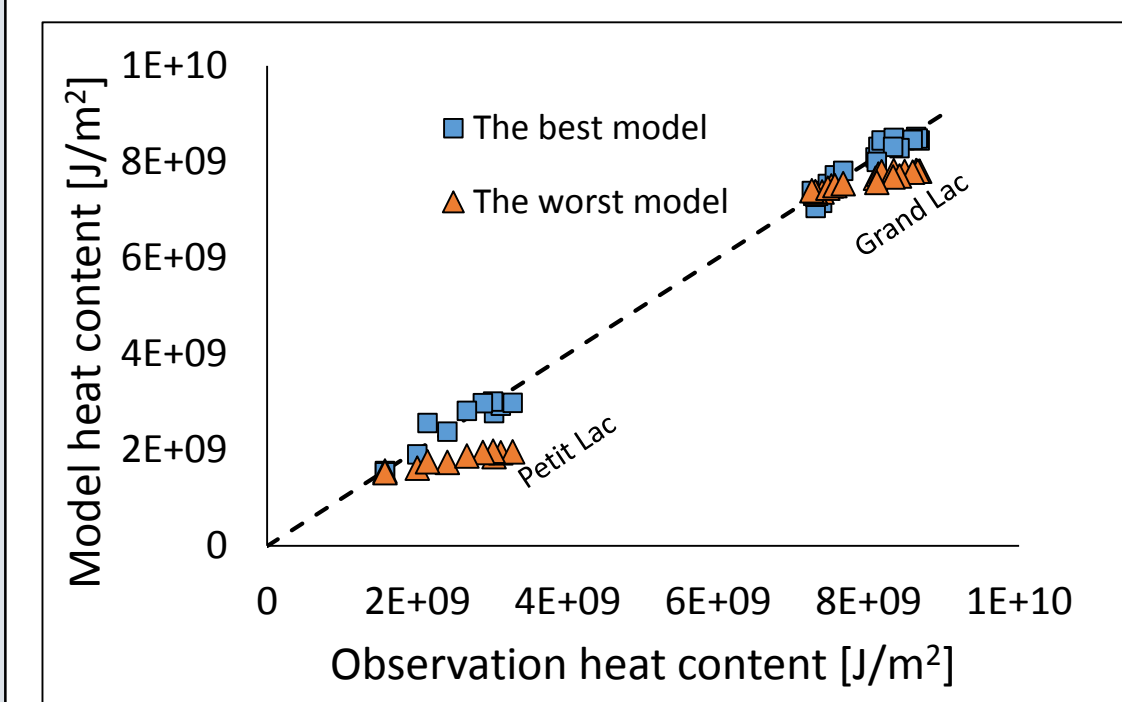


Figure 3 Comparison of the best ($Q_{tot,12313}$) and the worst ($Q_{tot,33123}$) total heat flux models, compared with 1:1 line.

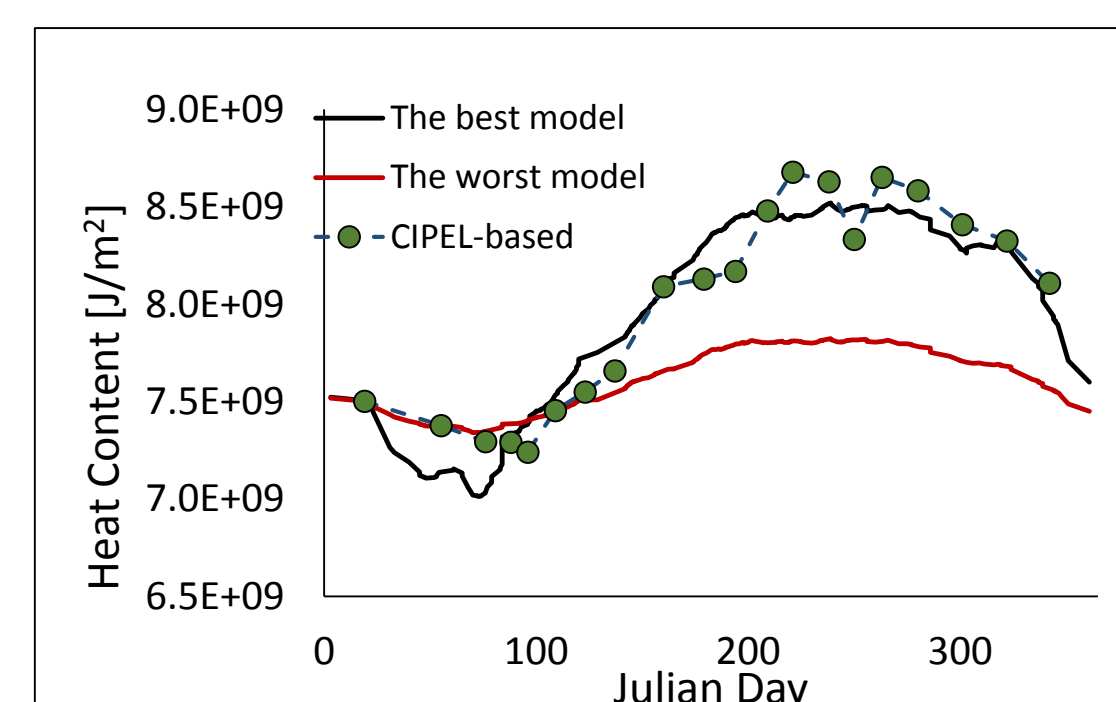


Figure 4 Temporal evolution of the lake heat content at the SHL2 station, observation vs model results.

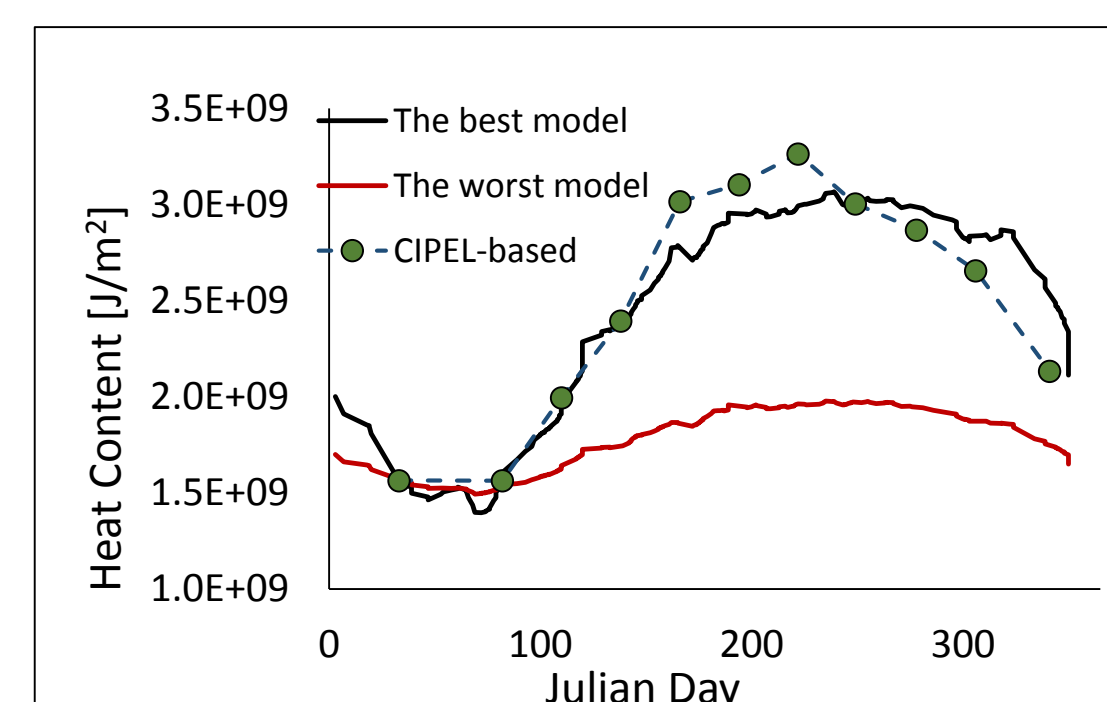


Figure 5 Temporal evolution of the lake heat content at the GE3 station, observation vs model results.

4. Results: Surface heat flux spatial patterns

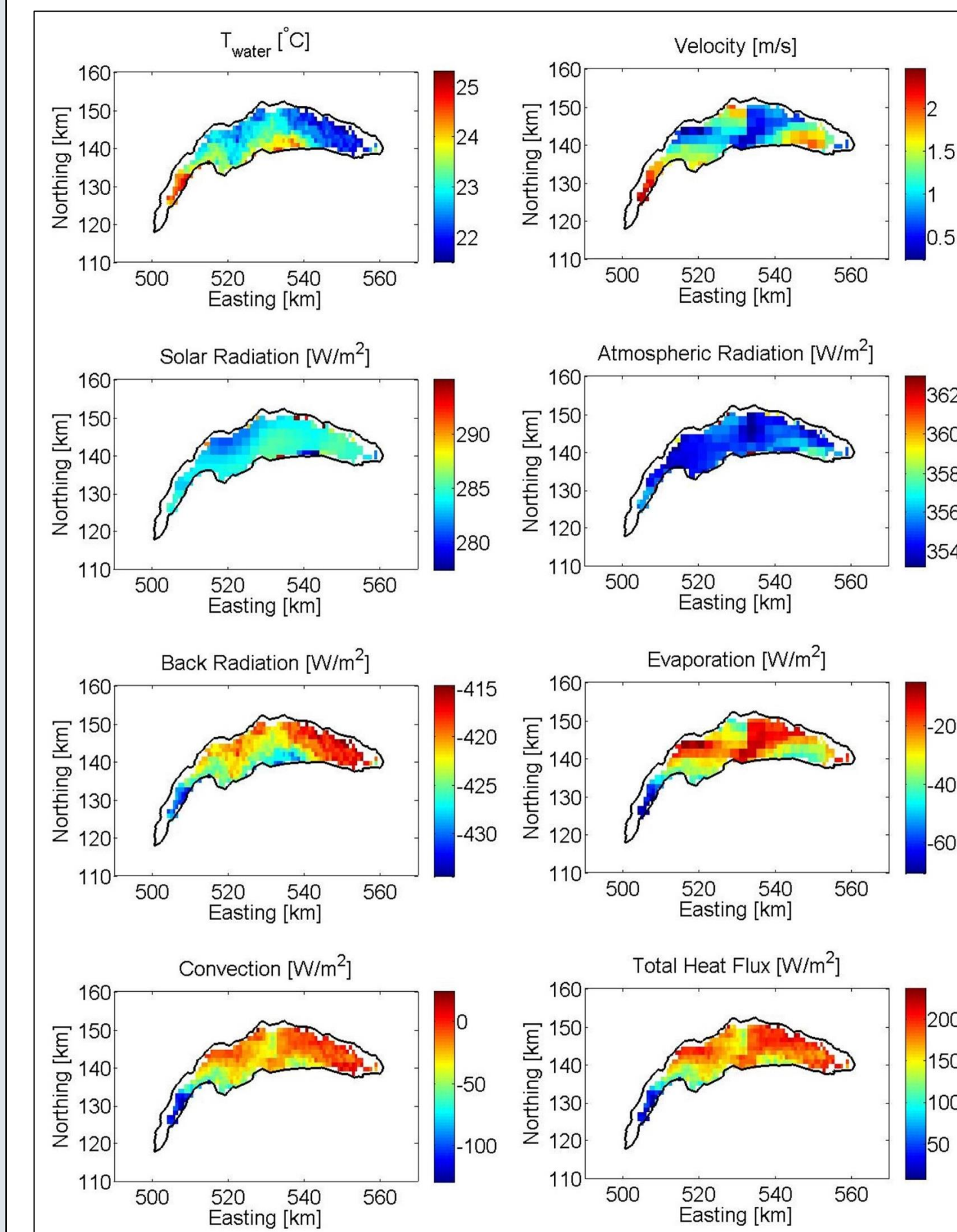


Figure 6 Example of LSWT (AVHRR satellite data), U_{10} (COSMO-2 data) as well as surface heat flux patterns of Lake Geneva. The results are from the best model for 15 July 2010. Patterns in the total surface heat flux are mainly due to LSWT and wind speed spatial variation. Preliminary observations show that the total heat flux spatial patchiness is more influenced by evaporation and convection terms whilst the radiation terms are dominant terms in its temporal variation.

5. Conclusions and Outlook

- An optimal bulk model was found for estimating the surface heat flux of Lake Geneva. This model was used to characterize the variability of the lake surface heat exchange, and to explain factors affecting temporal variability.
- The modeling results revealed that the LSWT and wind forcing are dominant factors underlying Lake Geneva's surface heat flux spatial variations, while its temporal variability is mainly due to the radiation and air temperature changes.
- Outlook: There is a good correlation between the total heat flux spatial patterns and convection/evaporation spatial patterns in the majority of observations. Quantification of these correlations and the role of seasonality is underway.

References

- [1] Fink, G. M. Schmid, B. Wahl, T. Wolf, and A. Wüest, 2014: Heat flux modifications related to climate-induced warming of large European lakes. *Water Resources Res.*, 50, 2072-2085.
- [2] Delft3D-FLOW, User Manual 2011, Version: 3.15, Revision: 17474. <http://www.deltaresystems.com/hydro/product/621497/delft3dsuite>.
- [3] Livingstone, D. M., and D. M. Imboden, 1989: Annual heat balance and equilibrium temperature of lake Aegeri, Switzerland. *Aquatic Sciences*, 51/4, 351-369.
- [4] Murakami, M., Y. Onisishi and H. Kunishi, 1985: A numerical simulation of the distribution of water temperature and salinity in the Seto Inland Sea. *Journal of the Oceanographical Society of Japan*, 41, 221-224.